Nanopore Facilitated Monohydrocalcitic Amorphous Calcium Carbonate Precipitation

Katharine Page,[a] Andrew G. Stack,[b] and Hsiu-Wen Wang*[b]*

[a]Neutron Scattering Division and [b]Chemical Sciences Division, Oak Ridge National Laboratory, Oak Ridge, TN 37831, USA.

KEYWORDS Amorphous materials, polymorphism, nucleation, X-ray diffraction, carbon storage.

ABSTRACT Predicting the precipitation of solids is important in both natural systems and subsurface energy applications. The factors controlling reaction mechanisms, phase selection and conversion between phases receive particular attention. In this contribution the precipitation and growth of an amorphous calcium carbonate species from flowing aqueous solution in a nanoporous controlled pore glass is followed *in situ* with differential X-ray pair distribution function analysis. The local atomic structure of this phase indicates monohydrocalcite-like pair-pair correlations, yet is functionally amorphous because it lacks long-range structure. The unexpected occurrence of synthetic proto-monohydrocalcite amorphous calcium carbonate, precipitated from a solution undersaturated with respect to published solubilities, suggests that nanopore confinement facilitates formation of an amorphous phase at the expense of more favorable crystalline ones. This result illustrates that confinement and interface effects are

important physical factors influencing mineral nucleation behavior in natural and geological systems.

Introduction

There are five crystalline calcium carbonate minerals: the three anhydrous phases, calcite, aragonite, and vaterite; and the two hydrous phases, monohydrocalcite and ikaite. Some of these phases are ubiquitous in the subsurface and play a central role in energy-relevant applications such as scale formation during oil and gas production, carbon sequestration, and transport of toxic metal contaminants. Amorphous calcium carbonate, ACC ($CaCO_3 \cdot nH_2O$) is significant in biomineral formation, and is recognized as a likely precursor in the formation of crystalline carbonate minerals based on the high energy barrier for calcite nucleation in accordance with classical nucleation theory[1,2] (approximately 100 kJ/mol for formation of critical radii[3]). At the same time, there is significant evidence that biogenic ACC exists in a variety of polyamorphic forms; that is, various forms exhibit short-range order matching local atomic bonding of specific crystalline polymorphs.[2,4,5] It has been shown that synthetic forms of ACC can be made: aragonitic-ACC by applied pressure,[6] proto-calcite and proto-vaterite by slow-dosing fixed pH method[2,7] monohydrocalcitic-amorphous (basic) calcium carbonate (A(B)CC) by fast centrifugal mixing,[8] and ACC without clear crystalline analog.[9] It has also been shown that a rich amorphous polytypism and stabilization mechanism exist in additive stabilized ACCs.[10-16] It has been suggested that these various "pre-structured" forms could determine crystallization pathways,[2,10] yet recent results point to the contrary.[14,15,17] Although the presence of specific protocrystalline structural motifs is still under debate, more recent results point to the pH effect and cooperation of hydroxide ions (in addition to water molecules) into synthetically pure A(B)CC as the key factors in stabilizing and controlling

atomic scale changes in A(B)CC structure.[7,17] The use of (m)ethanol is also known to assist in stabilizing ACC nanoparticles precipitated directly from homogeneous calcium carbonate solution.[18-20]

Mineral precipitation within localized environments is fundamental to biomineralization and subsurface heterogeneous nucleation processes, providing an alternative mechanism for stabilizing amorphous precursors. For example, it has been demonstrated that lipid vesicles can extend the lifetime of ACC before crystallization[21], and confinement alone provide an effective inorganic mimic of spicule environment to stabilize ACC.[22,23] The presence of porous media (a certainty in the subsurface) is a key factor that will affect precipitation reactions, and on that subject much contradictory evidence has arisen, including concepts for heterogeneous precipitation across all surface area regardless of pore size, for nucleation suppression in small pores, and precipitation enhancement in small pores.[3] Stack et al. previously demonstrated via *in situ* small angle X-ray scattering (SAXS) that growth of $CaCO_3$ in nanoporous silica matrix displays surface chemistry and pore-size dependent effects.[24] Key uncertainties in debates over crystallization are the structure of initial nuclei, and how those structures develop during crystal growth. Here we explore the nature of calcium carbonate precipitation and growth in confined nanopores with *in situ* X-ray pair distribution function (PDF) measurements, increasingly used for structural studies of adsorbed, absorbed, or precipitated species on the surfaces of porous and nanocrystalline materials.[e.g. 25-28] Our results reveal the formation of a monohydrocalcite-like amorphous calcium carbonate from a moderate pH (8.4) solution that is undersaturated with respect to monohydrocalcite, ikaite, and ACC phases (Table 1). Its occurrence inside pores demonstrate alternative mechanisms of stabilization and control over the structure of initial nuclei. This observation has direct

implications on the importance of confinement in the thermodynamic and kinetic control of mineral nucleation in geological fluid-pore environments.

Experimental Section

In-situ X-ray PDF measurements were completed at the 11-ID-B instrument, at The Advanced Photon Source at Argonne National Laboratory[29] utilizing a beam size of 500 μm by 500 μm, a photon energy of 58.65 keV (λ = 0.2114 Å), and a Perkin Elmer amorphous silicon image plate detector. A controlled-pore glass with nominal nanopore diameter of 24 nm (CPG-240, Millipore, Lincoln Park, NJ, USA), was loaded in a 1.6 mm polyaniline capillary fitted with a frit and ferrule with a 2 μm sieve, encased with a compression ring, and connected to a peristaltic pump (Masterflex model no. 7520-50) through Tygon tubing. The assembly was mounted vertically in the X-ray beam and aligned. The experimental setup is shown in Figure S1.

A 1 L growth solution with a constant supersaturation of calcium carbonate was prepared immediately prior to the start of the experiment by mixing 964.5 mL of DI water with 18.5 mL of 0.1M $CaCl_2$ and 17.0 mL of 0.1M $NaHCO_3$ stock solutions (all stock solutions were equilibrated with the atmosphere $CO_{2(g)}$ for a week). The composition of the growth solution was determined to be $[Ca^{2+}]/[CO_3^{2-}]$ ratio of 90±1 and pH of 8.40±0.01 at 25 °C, estimated using the PHREEQC code with the LLNL database.[30] The saturation index (SI) of this solution relative to the known carbonate phases is provided in Table 1. Solution was flowed through the CPG-filled column at a flow rate of 100 mL/h. Data was collected in 10 minute intervals starting from the time the fluid front passed through the cell. Data for samples of crystalline calcite, aragonite, and monohydrocalcite, as well as neat synthetic A(B)CC were collected for reference. Further details of the experimental setup are provided in the Supporting Information.

Table 1. Saturation Index (SI) of the $CaCO_3$ growth solution used in this study with respect to known carbonate phases. SI = $\log(a_{Ca}a_{CO3} / K_{sp})$, and K_{sp} = solubility product.

Phase	**– log(K_{sp}) at 25 °C**	**SI**
Calcite	8.48(2)[31,32]	0.74(2)
Aragonite	8.34(2)[31,32]	0.60(2)
Vaterite	7.91(2)[32]	0.17(2)
Monohydrocalcite	7.15(10)[33]	-0.6(1)
Ikaite	7.46(1)[33], 6.58(2)[34]	-0.28(1), 1.16(2)
ACC	6.39(2)[33,35], 6.0(3)[36]	-1.35(2), -1.7(3)
ACC I & II	~ 7.51[2] & 7.422[2]	~ -0.23 & -0.32

Results and Discussion

Time-resolved X-ray PDFs, G(r), of a carbonate solution flowing through a CPG substrate are shown in Figure 1. The as-collected data in Figure 1(c) is dominated by the structural correlations of the CPG framework, corresponding to an amorphous SiO_2 network. Difference PDFs in Figure 1(b), ΔG(r), created by subtracting the first 10 minutes of collected data from each dataset, exhibit both negative (corresponding to shifting amounts of CPG in the X-ray beam) and positive (corresponding to carbonate species) pair-pair correlations growing with time. The amount of subtracted SiO_2 background is adjusted to produce the final series of normalized ΔG(r) shown in Figure 1(a). The first few correlations match known carbonate, calcium, and water-oxygen pair-pair distances (e.g., intramolecular C-O_c at ~1.3 Å and O_c-O_c at ~2.4 Å, and intermolecular Ca-O_c/O_w at ~2.4 Å, etc.). The observed structure is amorphous:

there are no structural correlations above 8 Å in real space. This agrees well with the absence of lattice fringes observed with transmission electron microscopy (TEM) for carbonate solution flow precipitates in CPG.[24]

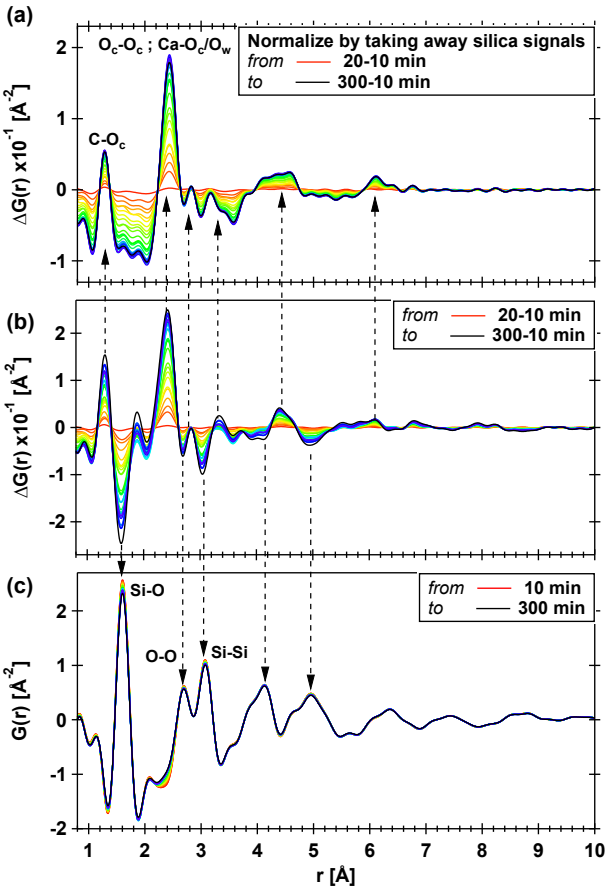

Figure 1. (a) Normalized difference PDFs every 10 minutes relative to the first dataset, corrected for diminishing signal from the CPG substrate. (b) Raw difference PDFs. (c) Total time resolved experimental X-ray PDFs as a function of time. In all panels the first data set (completed at 10 minutes after the start of flow) is shown in red, and the final data set (collected between 290 and 300 minutes) is shown in black. Data in both (a) and (b) are shown at 10 times scale relative to (c). Arrows indicate relationships between datasets.

Figure 2(a) shows the final 300 minute data set for the precipitated phase compared with data collected for neat A(B)CC, which we have reported[8] to qualitatively match ACC X-ray PDF data reported by e.g., Tobler et al.[17], Michel et. al[37] and modeled by Goodwin et. al.[38] While the precipitated data share some gross features with neat A(B)CC, the intensity and width of the first ($C\text{-}O_c$) correlation are poorly matched, and position and intensities of correlations between 3.5 Å and 5.5 Å (attributed to groups of Ca-Ca and $Ca\text{-}O_C/O_w$ correlations), significantly vary. Is the precipitated ACC an amorphous polytype of a particular crystalline phase instead? Figure 2(b) shows refinement results for the local atomic structure of the collected amorphous precipitate data using the crystalline polymorph models shown in Supporting Information Figure S2. All models match the approximate location and shape of the $C\text{-}O_c$ correlation at 1.3 Å and the $Ca\text{-}O_c/O_c\text{-}O_c$ correlations at 2.4 Å. However, the match to the data for the bulk monohydrocalcite model agrees remarkably well with the precipitate data across the complete range, and is also a significant improvement relative to agreement with neat A(B)CC data displayed in Figure 2(a). The scattering length density fitted in the previous SAXS analysis[24] was found to be close to that of monohydrocalcite, rather than calcite, and was attributed to a simplistic model in the original work. Since our local structure observations corroborate well TEM observations and SAXS modeling for a similar experimental setup, we conclude that the precipitating phase can be described as monohydrocalcitic-ACC.

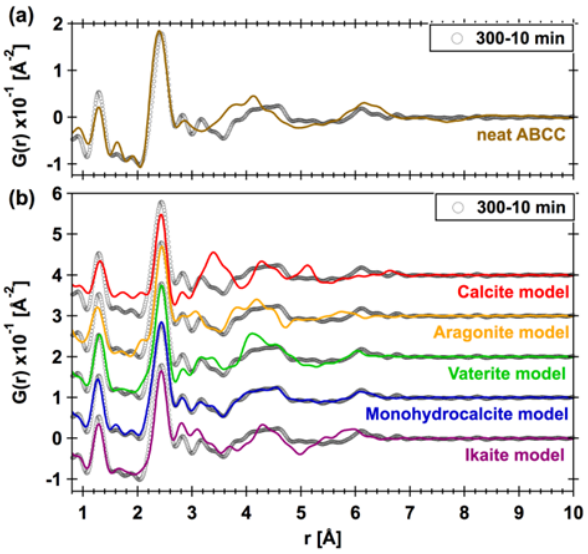

Figure 2. (a) A comparison of the precipitated phase data at 300 minutes (open grey circles) to an amorphous basic calcium carbonate data set (mustard line). (b) Comparison of the data with structure refinement results based on models from Figure S2.

The saturation index (SI) of the growth solution (Table 1) indicates that thermodynamically favorable growth conditions are present for calcite, aragonite, or vaterite, but not monohydrocalcite, ikiate or ACCs. Monohydocalcite is well known to be metastable with respect to calcite and vaterite,[39] though it has been observed in air conditioning systems,[40] in moonmilk deposits in caves (water/spray environments),[41] and in biological systems,[42-44] and can be formed via Mg-rich ACC precursors.[10,45] The presence of Mg in solution is known to inhibit the formation of vaterite and calcite, preferring direct incorporation into monohydrocalcite.[46] The formation of monohydrocalcitic-ACC under (Mg-free) flow conditions in nanopores is therefore a surprising result. This opens the intriguing question of whether nanopores allow amorphous phases to form at lower supersaturations than through other pathways.

Time-resolved measurements enable further examination of the nature of monohydrocalcitic-ACC precipitation in CPG. Figure 3 displays the time dependence of refinement model parameters and goodness of fit, R_w, for the series, along with the scale factor needed to remove changing silica intensities (see Supporting Information). The nearly constant correlation length scale and the minimal changes in R_w indicate a consistent amorphous monohydrocalcitic motif with time (Fig. 3(b)). The amount of precipitated material (as reflected by the refined scale factor) indicates nearly linear accumulation over the first 150 minutes, slowing beyond approximately 200 minutes (Fig. 3(a)). The observed cessation of growth, along with the earlier SAXS results showing that ACC never completely fills available pores,[24] suggests the precipitate reaches a steady state in silica nanopores, perhaps as an interfacial thin layer. If this amorphous monohydrocalcitic-ACC were a viable precursor for calcite in this environment, it might be expected to convert to calcite but such growth behaviors are not observed over the limited time-scales in this experiment or in previous work.[24]

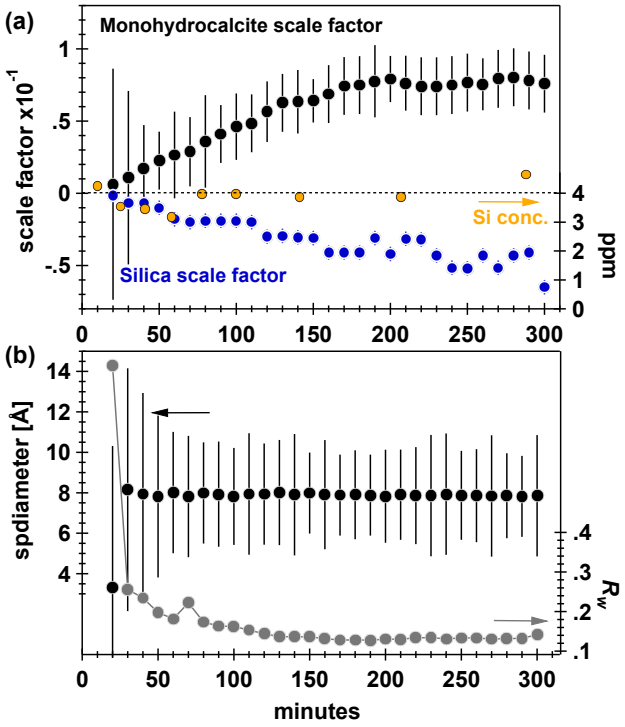

Figure 3. (a) The refined scale factor (in black) of the monohydrocalcite structural model from each data set, along with the scale factor applied to remove silica signal (in blue) from the final ΔG(r). The measured concentration of Si in solution is shown in yellow in ppm. (b) The refined correlation length scale (as spdiameter) and final R_w values from each fit.

This surprising result may be qualitatively rationalized using classical nucleation theory applied to heterogeneous nucleation, in which overall thermodynamic stability of a nucleus is expressed in terms of bulk and surface free energies.[47] The latter is a function of three component interfacial energies: substrate-precipitate, precipitate-solution, and substrate-solution. When the substrate surface area to solution volume ratio is high, the substrate-precipitate interfacial energy may drive phase selection. It could be that the ACC-CPG interfacial energy is sufficiently low, relative to the interfacial energies of the crystalline phases to CPG, that it overcomes the more favorable bulk free energy of the crystalline phases. Anion exclusion may be an alternative explanation. That is, the negative surface charges expected on CPG at pH 8.4 create a local nanopore environment where calcium-to-carbonate ratios are much higher than in the original solution.[3] Very high calcium-to-carbonate ratios have produced flocs of material out of solution at similar pH values.[48] It is possible that contradictory theories for the pore-size dependence of precipitation could be resolved accounting for these substrate-precipitate interactions, and the surface area to fluid volume ratio of the porous medium.

Summary and Conclusions

We have observed a monohydrocalcitic-ACC precipitate forming within a CPG substrate under solution conditions thermodynamically favoring calcite, aragonite, or vaterite formation, but not ACC or monohydrocalcite. The observation that the presence of nanopores (high ratio of

substrate surface area to solution volume) can affect carbonate phase selection and growth has obvious implications for precipitation in the subsurface, suggesting that solubility product alone, or kinetic measurements of nucleation/growth in open solution, are not sufficient to predict which phase(s) will form in confined environments. Our results demonstrate another key factor in determining structural formation and stability of ACC phases/precursors. We summarize in Figure 4, a schematic diagram, on the various reported chemical and physical controls identified in the literature for ACC formation and stability.

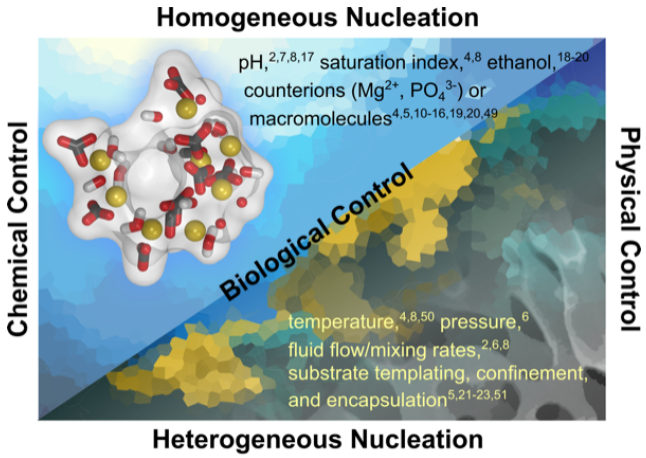

Figure 4

Figure 4. Chemical and physical factors reported to impact or improve the formation or stabilization of amorphous calcium carbonates (representative references are noted). Both chemical and physical factors are harnessed in the biological control of phases.

We have also demonstrated the sensitivity of difference PDF to tracking the identity, rate, and size of very small precipitates forming out of flowing carbonate solution in CPG: a reasonable proxy for studying precipitation in rock. The methods can readily be modified to investigate the influence of flow rate, temperature, pore size, saturation levels, pore-wall chemistry, additives, etc. on the precipitation, growth and stabilization of metastable phases. It would be fascinating to

try the same with neutron PDF, where the behavior and influence of (heavy) water on these processes may be observed.

ASSOCIATED CONTENT

Supporting Information. Details of experiment procedures and crystalline reference material datasets, refinements, and models. This material is available free of charge via the Internet at http://pubs.acs.org.

AUTHOR INFORMATION

Corresponding Author

*pagekl@ornl.gov

*wang3@ornl.gov

Author Contributions

The manuscript was written through contributions of all authors. All authors have given approval to the final version of the manuscript.

ACKNOWLEDGMENT

The work by all authors was supported under the Department of Energy's Office of Basic Energy Sciences. K.P. was supported through the U.S. Department of Energy, Office of Science, Office of Basic Energy Sciences, Early Career Research Program Award KC040602. H.-W.W. and A.G.S. were supported through the U.S. Department of Energy, Office of Science, Office of Basic Energy Sciences, Chemical Sciences, Geosciences, and Biosciences Division. Research at the 11-ID-B beamline used resources of the Advanced Photon Source, a U.S. Department of

Energy (DOE) Office of Science User Facility operated for the DOE Office of Science by Argonne National Laboratory under Contract No. DE-AC02-06CH11357. The authors thank Kevin Bayer for technical support at the 11-ID-B beamline. The monohydrocalcite sample (NMNH 135404 00) is from the mineral collection of the Department of Mineral Sciences, Smithsonian Institution.

REFERENCES

1. Raiteri, P.; Gale, J. D. Water Is the Key to Nonclassical Nucleation of Amorphous Calcium Carbonate. *J. Am. Chem. Soc*. **2010**, *132*, 17623-17634.
2. Gebauer, D.; Volkel, A.; Colfen, H. Stable Prenucleation Calcium Carbonate Clusters. *Science* **2008**, *322*, 1819-1822.
3. Stack, A. G. Precipitation in Pores: A Geochemical Frontier. *Rev. Mineral. Geochem*. **2015**, *80*, 165-190.
4. Cartwright, J. H.; Checa, A. G.; Gale, J. D.; Gebauer, D.; Sainz-Diaz, G. I. Calcium Carbonate Polyamorphism and its Role in Biomineralization: How Many Amorphous Calcium Carbonates are There? *Angew. Chem. Int. Ed*. Engl. **2012**, *51*, 11960-11970.
5. Weiner, S.; Levi-Kalisman, Y.; Raz, S.; Addadi, L. Biologically Formed Amorphous Calcium Carbonate. *Connect Tissue Res.*, **2003**, *44*, 214-218.
6. Fernandez-Martinez, A.; Kalkan, B.; Clark, S. M.; Waychunas, G. A. Pressure-induced Polyamorphism and Formation of 'Aragonitic' Amorphous Calcium Carbonate. *Angew. Chem. Int. Ed.* **2013**, *52*, 8354-8357.
7. Gebauer, D.; Gunawidjaja, P. N.; Ko, J. Y.; Bacsik, Z.; Aziz, B.; Liu, L.; Hu, Y.; Bergstrom, L.; Tai, C. W.; Sham, T. K.; Eden, M.; Hedin, N. Proto-calcite and Proto-vaterite in Amorphous Calcium Carbonates. *Angew. Chem. Int. Ed. Engl*. **2010**, *49*, 8889-8891.
8. Wang, H.-W.; Daemen, L. L.; Cheshire, M. C.; Kidder, M. K.; Stack, A. G.; Allard, L. F.; Neuefeind, J. C.; Olds, D.; Liu, J.; Page, K. Synthesis and Structure of Synthetically Pure and Deuterated Amorphous (Basic) Calcium Carbonates. *Chem. Commun.* **2017**, *53*, 2942-2945.
9. Khouzani, M. F.; Chevrier, D. M.; Güttlein, P.; Hauser, K.; Zhang, P.; Hedin, N; Gebauer, D. Disordered Amorphous Calcium Carbonate from Direct Precipitation. *CrystEngComm* **2015**, *17*, 4842-4849.
10. Raymond, S. K.; Lam, J. M.; Charnock, A. L.; Meldrum, F. C. Synthesis-Dependent Structural Variations in Amorphous Calcium Carbonate. *CrystEngComm*, **2007**, *9*, 1226–1236.
11. Guillemet, B.; Faatz, M.; Gröhn, F.; Wegner, G.; Gnanou, Y. Nanosized amorphous calcium carbonate stabilized by poly (ethylene oxide)-b-poly (acrylic acid) block copolymers. *Langmuir* **2006**, *22*, 1875-1879.
12. Gal, A.; Weiner, S.; Addadi, L. The stabilizing effect of silicate on biogenic and synthetic amorphous calcium carbonate. *J. Am. Chem. Soc.* **2010**, *132*, 13208-13211.

13. Kellermeier, M.; Melero-Garcia, E.; Glaab, F.; Klein, R.; Drechsler, M.; Rachel, R.; García-Ruiz, J. M.; Kunz, W. Stabilization of amorphous calcium carbonate in inorganic silica-rich environments. *J. Am. Chem. Soc.* **2010**, *132*, 17859-17866.
14. Kababya, S.; Gal, A.; Kahil, K.; Weiner, S.; Addadi, L.; Schmidt, A. Phosphate–water interplay tunes amorphous calcium carbonate metastability: spontaneous phase separation and crystallization vs stabilization viewed by solid state NMR. *J. Am. Chem. Soc.* **2015**, *137*, 990-998.
15. Alberic, M.; Bertinetti, L.; Zou, Z.; Fratzl, P.; Habraken, W.; Politi, Y. The Crystallization of Amorphous Calcium Carbonate is Kinetically Governed by Ion Impurities and Water. *Adv Sci (Weinh)* **2018**, *5*, 1701000.
16. Koishi, A.; Fernandez-Martinez, A.; Ruta, B.; Jimenez-Ruiz, M.; Poloni, R.; di Tommaso, D.; Zontone, F.; Waychunas, G. A.; Montes-Hernandez, G. Role of Impurities in the Kinetic Persistence of Amorphous Calcium Carbonate: A Nanoscopic Dynamics View. *The Journal of Physical Chemistry C* **2018**, *122*, 16983-16991.
17. Tobler, D. J.; Rodriguez-Blanco, J. D.; Sørensen, H. O.; Stipp, S. L. S.; Dideriksen, K. Effect of pH on Amorphous Calcium Carbonate Structure and Transformation. *Cryst. Growth Des.* **2016**, *16*, 4500-4508.
18. Chen, S. F.; Colfen, H.; Antonietti, M; Yu, S. Ethanol Assisted Synthesis of Pure and Stable Amorphous Calcium Carbonate Nanoparticles. *Chem. Commun.* **2013**, *49*, 9564-9566.
19. Lei, Z.; Sun, S.; Wu, P. Ultrafast, Scale-Up Synthesis of Pure and Stable Amorphous Carbonate Mineral Nanoparticles. *ACS Sustainable Chemistry & Engineering* **2017**, *5*, 4499-4504.
20. Sun, R.; Zhang, P.; Bajnoczi, E. G.; Neagu, A.; Tai, C. W.; Persson, I.; Stromme, M.; Cheung, O. Amorphous Calcium Carbonate Constructed from Nanoparticle Aggregates with Unprecedented Surface Area and Mesoporosity. *ACS Appl. Mater. Interfaces* **2018**, *10*, 21556-21564.
21. Tester, C. C.; Brock, R. E.; Wu, C.-H.; Krejci, M. R.; Weigand, S.; Joester, D. In vitro Synthesis and Stabilization of Amorphous Calcium Carbonate (ACC) Nanoparticles within Liposomes. *Cryst. Eng. Comm.* **2011**, *13*, 3975 – 3978.
22. Stephens, C. J.; Ladden, S. F.; Meldrum, F. C.; Christenson, H. K. Amorphous Calcium Carbonate is Stabilized in Confinement. *Adv. Funct. Mater.* **2010**, *20*, 2108-2115.
23. Ihli, J.; Wong, C. W.; Noel, E. H.; Kim, Y. Y.; Kulak, A. N.; Christenson, H. K.; Duer, M. J.; Meldrum, F. C. Dehydration and Crystallization of Amorphous Calcium Carbonate in Solution and in Air. *Nat. Commun.* **2014**, *5*, 3169.
24. Stack, A. G.; Fernandez-Martinez, A; Allard, L. F.; Banuelos, J. L.; Rother, G.; Anovitz, L. M.; Cole, D. R.; Waychunas, G. A. Pore-size-dependent Calcium Carbonate Precipitation Controlled by Surface Chemistry. *Environ. Sci. Technol*. **2014**, *48*, 6177-6183.
25. Chupas, P. J.; Chapman, K. W.; Jennings, G.; Lee, P. L.; Grey, C. P. Watching Nanoparticles Grow: The Mechanism and Kinetics for the Formation of TiO_2-Supported Platinum Nanoparticle. *J. Am. Chem. Soc.* **2007**, *129*, 13822–13824.
26. Jensen, K. M. Ø.; Christenson, M.; Juhas, P.; Tyrsted, C.; Bøjeson, E. D.; Lock, N.; Billinge, S. J. L.; Iverson, B. B. Revealing the Mechanisms behind SnO_2 Nanoparticle Formation and Growth During Hydrothermal Synthesis: an in situ Total Scattering Study. *J. Am. Chem. Soc*. **2012**, *134*, 6785-6792.

27. Kim, H.; Karkamkar, A.; Autrey, T.; Chupas, P.; Proffen, T. Determination of Structure and Phase Transition of Light Element Nanocomposites in Mesoporous Silica: Case study of NH_3BH_3 in MCM-41. *J. Am. Chem. Soc*. **2003**, *131*, 13749-13755.
28. Wang, H.-W.; Wesolowski, D. J.; Proffen, T.; Vlcek, L.; Wang, W. Allard, L. F.; Kolesnikov, A. I.; Feygenson, M; Anovitz, L. M.; Paul, R. L. Structure and Stability of SnO_2 Nanocrystals and Surface-Bound Water Species. *J. Am. Chem. Soc*. **2013**, 135, 6885-6895.
29. Chupas, P. J.; Qiu, X.; Hanson, J. C.; Lee, P. L.; Grey, C. P.; Billinge, S. J. L. Rapid-acquisition Pair Distribution Function (RA-PDF) Analysis. *J. Appl. Crystallogr.* **2003**, *36*, 1342-1347.
30. Parkhurst, D. L. User's Guide to PHREEQE—a Computer Program for Speciation, Reaction-path, Advective Transport, and Inverse Geochemical Calculations, US Geological Survey Water-Resources Investigations Report, 1995.
31. Morse, J. W.; Mackenzie, F. T. *Geochemistry of Sedimentary Carbonates*, **1990**, *48*, Elsevier.
32. Plummer, L. N.; Busenberg, E. The Solubilities of Calcite, Aragonite and Vaterite in CO_2-H_2O Solutions between 0 and 90°C, and an Evaluation of the Aqueous Model for the system $CaCO_3$-CO_2-H_2O. *Geochim. Cosmochim. Acta,* **1982**, *46*, 1011-1040.
33. Brečević, L.; Kralj, D. On Calcium Carbonates: from Fundamental Research to Application. *Croat. Chem. Acta*, **2007**, *80*, 467-484.
34. Bischoff, J. L; Fitzpatrick, J. A.; Rosenbauer, R. J. The Solubility and Stabilization of Ikaite ($CaCO_{3.6}H_2O$) from 0˚ to 25˚C: Environmental and Paleoclimatic Implications for Thinolite Tufa. *J. Geol.*, **1993**, 21-33.
35. Brečević, L.; Nielsen, A. E. Solubility of Amorphous Calcium Carbonate. *J. Cryst. Growth***, 1989**, *98*, 504-510.
36. Ogino, T.; Suzuki, T.; Sawada, K. The Formation and Transformation Nechanism of Calcium Carbonate in Water. *Geochim. Cosmochim. Acta*, **1987**, *51*, 2757-2767.
37. Michel, F. M.; MacDonald, J.; Feng, J.; Phillips, B. L.; Ehm, L.; Tarabrella, C.; Parise, J. B.; Reeder, R. J. Structural Characteristics of Synthetic Amorphous Calcium Carbonate. *Chem. Mater*. **2008**, *20*, 4720-4728.
38. Goodwin, A. L.; Michel, F. M.; Phillips, B. L.; Keen, D. A.; Dove, M.; Reeder, R. J. Nanoporous Structure and Medium-Range Order in Synthetic Amorphous Calcium Carbonate. *Chem. Mater.* **2010**, *22*, 3197-3205.
39. Hull, H; Turnbull, A. G. A Thermochemical Study of Monohydrocalcite. *Geochim. Cosmochim. Acta* **1973**, *37*, 685–694.
40. Marschner, H. Hydrocalcite ($CaCO_3H_2O$) and Nesquehonite ($MgCO_3$•$3H_2O$) in Carbonate Scales. *Science*, **1969**, *165*, 1119–1121.
41. Dahl, K.; Buchardt, B. J. Monohydrocalcite in the Arctic Ikka Fjord, SW Greenland: First Reported Marine Accurrence. *Sediment. Res.* **2006**, *76*, 460–471.
42. Catherine, H.; Skinner, K.; Osbaldiston, G. W.; Wilner, A. N. Monohydrocalcite in a Guinea Pig Bladder Stone, a Novel Occurrence. *Am. Mineral.* **1977**, *62*, 273 - 277.
43. Señorale-Pose, M.; Chalara, C.; Dauphin, Y.; Massard, P.; Pradel, P.; Marína, M. Monohydrocalcite in Calcareous Corpuscles of Mesocestoides Corti. *Exp. Parasitol.* **2007**, *118*, 54–58.
44. Garvie, L. A. J. Decay-induced Biomineralization of the Saguaro Cactus (Carnegiea Gigantea). *J. Am. Mineral.* **2003**, *88*, 1879-1888.

45. Wang, Y.-Y.; Yao, Q.-Z.; Zhou, G.-T.; Fu, S.-Q. Transformation of Amorphous Calcium Carbonate into Monohydrocalcite in Aqueous Solution: A Biomimetic Mineralization Study. *Eur. J. Mineral.* **2015**, *27*, 717-729.
46. Rodriguez-Blanco, J. D.; Shaw, S.; Bots, P.; Roncal-Herrero, T.; Benning, L. G. The Role of Mg in the Crystallisation of Monohydrocalcite. *Geochim. Cosmochim. Acta* **2014**, *127*, 204–220.
47. De Yoreo, J. J.; Vekilov, P. G. Principles of Crystal Nucleation and Growth. *Rev. Mineral. Geochem.* **2003**, *54*, 57-94.
48. Gebrehiwet, T. A.; Redden, G. D.; Fujita, Y.; Beig, M. S.; Smith, R. W. The Effect of the CO_3^{2-} to Ca^{2+} Ion Activity Ratio on Calcite Precipitation Kinetics and Sr^{2+} Partitioning. *Geochem. Trans.* **2012**, *13*, 1-11.
49. Gower, L. B. Biomimetic Model Systems for Investigating the Amorphous Precursor Pathway and its Role in Biomineralization. *Chem. Rev*. **2008**, *108*, 4551-4627.
50. Ihli, J.; Kulak, A. N.; Meldrum, F. C. Freeze-drying Yields Stable and Pure Amorphous Calcium Carbonate (ACC). *Chem. Commun.* **2013**, *49*, 3134-3136.
51. Pouget, E. M.; Bomans, P. H.; Goos, J. A.; Frederik, P. M.; de With, G.; Sommerdijk, N. A. The Initial Stages of Template-Controlled $CaCO_3$ Formation Revealed by Cryo-TEM. *Science* **2009**, *323*, 1455-1458.

TOC Graphic

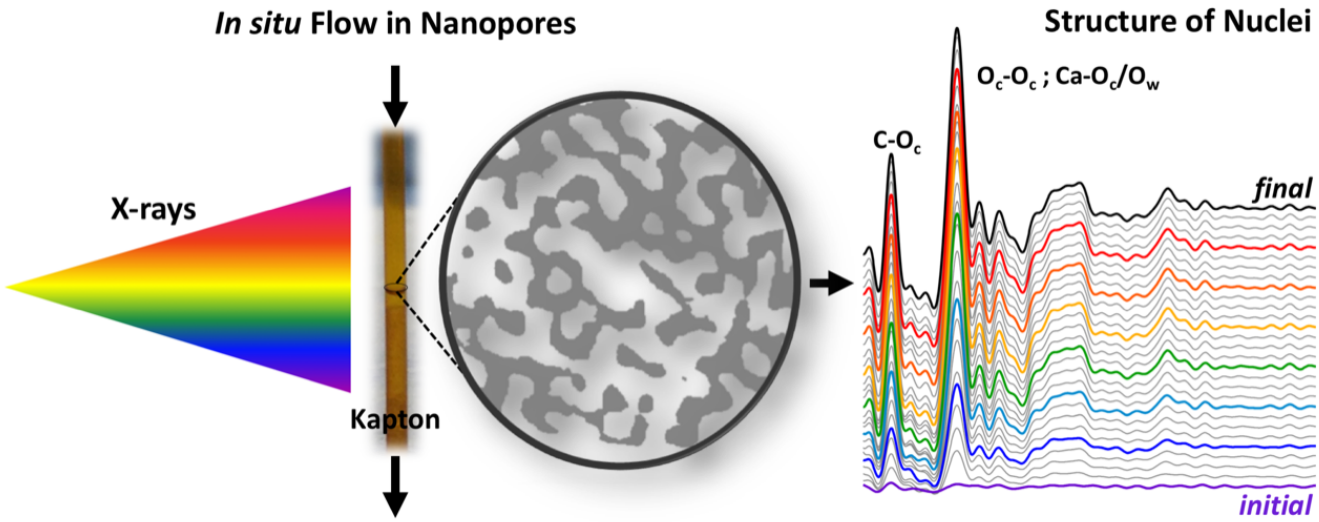

The unexpected precipitation of monohydrocalcite-like amorphous calcium carbonate from a solution undersaturated with respect to published solubilities, suggests that pore confinement facilitates formation of an amorphous phase at the expense of more favorable crystalline ones.